Mechanical Characterization of Insulation Materials During Thermal Battery Manufacturing

Laura D. Jacobs, Christopher R. Esquibel, Christine C. Roberts, Henry A. Padilla
Sandia National Laboratories
Albuquerque, NM, USA, 87185-0613
ldjacob@sandia.gov /1-505-844-8521

Abstract

The current study focuses on the material properties of insulation materials during manufacturing of thermal batteries. Manufacturing is characterized by cyclic loading, short stabilization times, and the relatively quick application of loads. Rigidized Fiberfrax, MinK, Zircal, Duraboard, Microtherm and WDS Shape insulation materials are subjected to cyclic loading using comparable closing forces employed in thermal batteries, and stress-strain curves are reported. Insulation stress responses show evidence of both elastic and irrecoverable plastic behavior which are important to understand for specifying insulation thicknesses and closing pressures in thermal battery designs.

Keywords

Insulation; Closing Force; Modeling

Introduction

Porous, ceramic felt-based insulation materials are utilized axially above and below the electrochemical cell stack in thermal batteries. In addition to heat insulation, the materials maintain a compressive stress on the stack that enables proper cell wetting with electrolyte during activation and prevents pellet slip during mechanical environments. Computational performance models using digital engineering tools are increasingly important for achieving shorter design cycles, fewer costly development builds, and more optimized designs. A crucial piece of thermal battery modeling is the mechanical response, however performance models for are hindered by poorly characterized material behavior. The mechanical response of thermal battery insulation materials throughout its lifetime, from manufacturing through deployment and use, is largely unknown, despite their crucial function to ensure thermal performance and mechanical robustness.

Insulation materials that are suitable for inclusion in thermal batteries must have mechanical properties that withstand multiple load and unload cycles characteristic of thermal battery manufacturing, as well as recovery strain properties to allow for sufficient stress to remain on the stack after the battery is fired, the electrolyte melts, and the stack shrinks in height. The ability to maintain pressure on the stack after activation is crucial to the battery being able to operate before and after being subjected mechanical environments, maintaining electrical contact throughout the stack during events, and the closing pressure of the thermal battery must be matched to the thickness of insulation materials in the battery design to achieve a weldable case height.

The mechanical behaviors of insulation that are key to modeling thermal batteries include the elastic modulus, cylic loading hysteresis, recovery strain, and time dependent stress relaxation. Elastic modulus is a common parameter used in modeling. Cylic loading hysteresis is key to understanding the state of the insulation during and after manufacturing. Recovery strain behavior is crucial for modeling what happens in the battery post activation. Stress relaxation is needed to model the stress on the stack for different durations of service life. .

The current study focuses on the material response of insulation materials during manufacturing. Manufacturing is characterized by cyclic loading, short stabilization times, and the relatively quick application of loads. The experiments in this study mimic load profiles during manufacturing.

Experimental Method

Materials: Six insulation materials, either commonly found in thermal batteries or potential candidates for future designs, were selected for investigation.

The materials selected were Fiberfrax stiffened with a rigid binder, Fiberfrax Duraboard, Thermal Ceramics TE-1400 Min-K, WDS Shape, Zircal, and Microtherm.

Sample Preparation: The samples were primarily 1” diameter cylinders that were fabricated using a punch. The Zircal and WDS Shape samples were not conducive to punch fabrication and, instead, were cut into approximate cubeswith a 1” square face. The thickness of the samples was dictated by the thickness of the stock material. The rigidized Fiberfrax was only 0.100” in thickness, so to ensure that the deformations were measurable, 5 samples were stacked vertically to make a 0.5” thick specimen. Dimensions and pictures of the samples can be found in Table 1. After the samples were cut out, they were then dried at 600˚C for 2 hours in a dryroom with a maximum dewpoint of -28˚C and stored in vacuum sealed bags until testing. The samples were tested in a radially unconfined state, which differs from the radially confined state in actual batteries. They were chosen to be tested in a radially unconfined state to get the material response to create material models.

Table 1. Sample Dimensions

Material	Picture	Dimensions
Duraboard	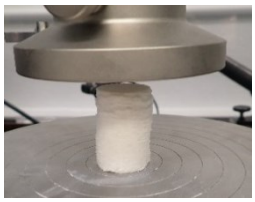	1” D x 2” H
Fiberfrax	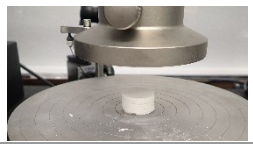	1” D x 0.1” H
Microtherm	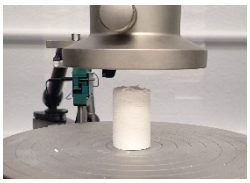	1” D x 1.575” H
MinK	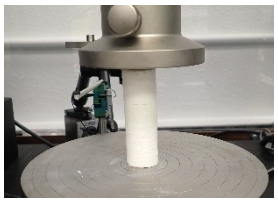	1”D x 3”H
WDS Shape	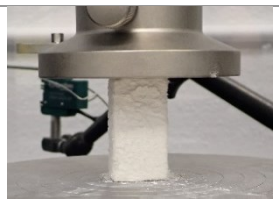	1” x 1” x 2”
Zircal	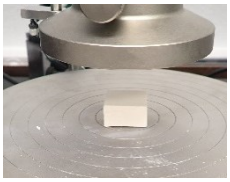	1” x 1” x 0.5”

Equipment: The experiments were conducted using an ADMET eXpert 2613 Dual Column Table Top Universal Testing System controlled using the MTEST Quattro Controller & Software. The test frame has the specifications shown in Table 2. A 10,000 lb load cell was used to make the force measurements. The ADMET was located in a dryroom with a maximum dewpoint of -28˚C to test the materials in their dry state.

An Epsilon Technology Group model 3540-012M-ST deflectometer was used to measure sample deformation. It uses a full bridge arrangement for strain measurement. It has a 12 mm range with => 0.25% linearity of full displacement range (linear up to 30 microns).

Table 2. ADMET Specifications [1]

Characteristic	Specification
Capacity	11,250 lb
Stroke	46 inches
Total Vertical Test Space	52 inches
Speed(max):	20 inches/min

Crush Tests: Crush tests were performed, wherein each sample was loaded at increasing levels until it failed to support the load. The goal of the crush test was to collect information on the yield andfracture strength of the materials to inform test conditions for cyclic load testing.

Cyclic Tests: The goal of the cyclic load test was to mimic the cyclic loading experienced by the insulation material during battery manufacture. The tests were strain controlled using a crosshead velocity of 2 inches/second. Three samples of each material were loaded to a peak force and held at a constant strain for 2 minutes, then unloaded to 10 lbs and held at a constant strain for 2 minutes, twice, followed by being loaded to the peak stress and held at a constant strain for 5 minutes and then unloaded to 10 lbs and held at a constant strain for 1 minute. The peak forces were selected so that the stresses on the samples were both representative of battery closing pressures and below the yield or fracture stress determined in the crush test. The peak stresses for each material can be found in Table 3.

Table 3. Maximum Stress Applied in Cyclic Load Tests

Material	Maximum stress (psi)
Duraboard	250
Fiberfrax	150
Microtherm	150
MinK	150
WDS Shape	100
Zircal	400

Experimental Results

Crush Tests: The primary goal of the crush tests was to investigate the material response and use it to inform the cyclic load tests. Figure 1 shows a wide variety of material behaviors and load magnitudes at failure for the insulation materials.

The Zircal and rigidized Fiberfrax (FF) were the two stiffest materials and could support the greatest stress. Both stiffened as the stress increased. MinK and WDS Shape had very similar mechanical behaviors. They had a linear stress-strain relationship until failure and the lowest failure loads of all the materials. The Min-K maximum loads were lower than observed in-situ. One possible explanation for this is that, in-situ, the material is radially confined. Future testing should include radial confinement. Also, during punch

fabrication, some of the material fibers were pulled, causing the samples to be curved rather than straight, and potentially weakening the material. The Microtherm was able to support more load than the WDS Shape and MinK and had an elastoplastic behavior. The Duraboard had a very long crushing phase which is nearly linear elastic prior to stiffening. A possible explanation for this behavior is that an initial densification must occur before the Duraboard supports larger stresses.

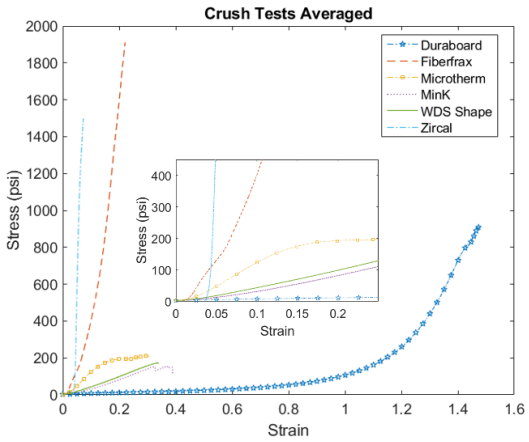

Figure 1. Averaged Stress-Strain Curves from Crush Tests

The cyclic load test maximum stress values were selected to be stresses that are typically found in batteries, but below the stresses where failure was observed. For the Microtherm, the stress was also limited to be lower than the point where the behavior was observed to transition to a plastic deformation. For the Duraboard, the stress was selected to be above the point where the material starts to stiffen.

Cyclic Load Tests: As with the crush tests, it is clear that the different materials span a broad range of behavior on the first cycle of loading. However, on the second and third cycles, the materials behave more similarly to one another. Time domain and stress-strain data both provide insight into the material behavior.

To compare stress-time data across materials, the stresses for were normalized by the maximum stress applied. The holding periods then all begin at the same normalized stress.

As can be seen in Figure 2, Fiberfrax exhibits stress relaxation during the hold after the maximum stress is applied. With each subsequent load and unload cycle, the amount of stress relaxation is reduced. Similar results were found in the other materials (Table 4) MinK and WDS Shape have the least amount of stress relaxation at about 3%. Microtherm and Zircal have about 6% stress relaxation. The Fiberfrax and Duraboard have about 20% stress relaxation in the first cycle and 15% in the later cycles. This is a significant drop in the amount of stress in the insulation materials and needs to be accounted for in the design of thermal batteries.

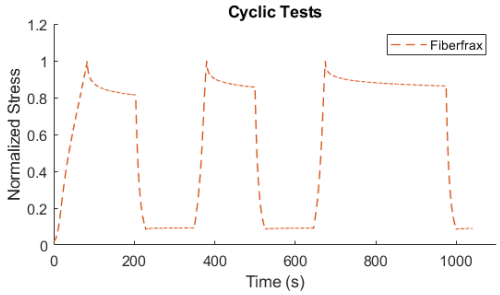

Figure 2. Normalized Stress vs Time During Cyclic Loading

Table 4. Percent Stress Relaxation per Cycle

Cycle	Dura-board	Fiber-frax	Micro-therm	Min-K	WDS Shape	Zircal
1	20.6	18.7	4.9	2.5	4.7	5.3
2	16.6	15.1	3.5	1.2	3.0	3.8
3	16.2	13.6	3.9	1.5	2.8	3.0

The first load and unload cycle for each of the materials, shown in Figure 3, crushed the material resulting in unrecoverable strain. The Duraboard experienced an order of magnitude more strain than the other five materials. The rigidized Fiberfrax and Microtherm had similar behavior in the first load and unload cycle. The MinK and WDS Shape had similar behaviors during the first load and unload cycle.

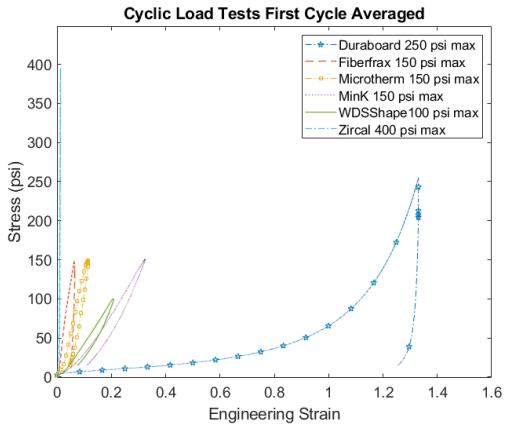

Figure 3. Stress-Strain Curve from the First Load-Unload Cycle

To compare the second and third cycles (Figure 4), the strains at the start of the second cycle were normalized to zero. The second and third load and unload curves produced more consistent behavior because the material went through an initial crushing during the first load. During the second load and unload cycles, the MinK and WDS Shape behaved similarly. They both exhibit more strain than the other materials.

Another parameter of interest for the predictive models is the modulus of elasticity when the materials are being loaded.

The elastic modulus during loading is calculated using the load portions of the stress-strain curves.

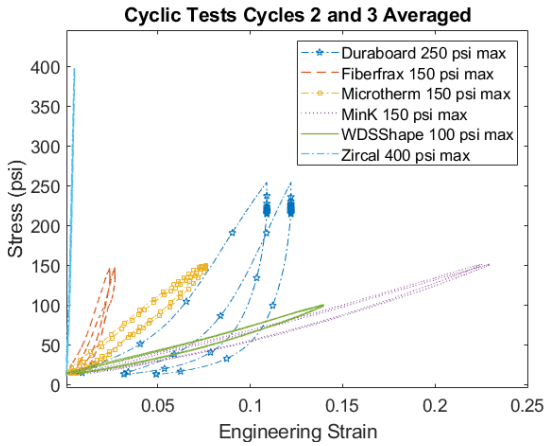

Figure 4. Stress-Strain Curve from the Second and Third Load-Unload Cycles

One of the critical parameters for predictive models is the recovery modulus which allows for predicting the stack force after activation. To determine the recovery stress-strain behavior of each material, the elastic modulus was calculated from the unload portions of the stress-strain curve in the second load cycle. The values for each of the materials are listed in Table 5. It is interesting to note that the moduli for the MinK and WDS Shape are nearly identical.

Table 5. Modulus of Elasticity for Loading and Unloading

Material	Maximum stress (psi)	Loading Elastic Modulus (psi)	Recovery Elastic Modulus (psi)
Duraboard	800	15750	50700
Fiberfrax	650	32020	68060
Microtherm	153	1840	2120
MinK	152	610	700
WDS Shape	100	544	676
Zircal	1000	96460	107430

Conclusions

This study begins the characterization of insulation materials found in thermal batteries. Six insulation materials were tested in representative manufacturing conditions. The materials exhibited a variety of materials properties and behaviors.

The stress-strain behavior of all the materials was different in the first cycle compared to the later cycles, due to an initial, irreversible crushing of the insulation material. The value of the recovery elastic modulus of the later cycles is representative of how the insulation materials would recover after the battery is activated, because in manufacturing the insulation goes through multiple load-unload cycles.

During this study, stress relaxation was observed during the relatively short hold times encountered during manufacturing. Some of the materials experienced as much as a 20% reduction in stress. Characterizing the stress relaxation is crucial for effective modeling of thermal batteries under mechanical loads. Additional studies are currently be performed that build upon the work done by Roberts et al [2] to characterize the stress relaxation over time of the insulation materials from this study in a battery representative atmosphere.

The current study should be expanded to look at multiple maximum stresses to determine if the material parameters are stress dependent. Additionally, tests with radial confinements that are representative of those found in a thermal battery would be useful in characterizing the materials.

Acknowledgements

The authors would like to thank Aaron Melad for his assistance with the ADMET, Marco Inzunza-Ibarra for his assistance with the deflectometer, Alan Harrington and Patrick Benavidez for preparing the test samples, Nicholas Streeter and John Taphouse for providing manufacturing loading information, and Nathaniel Johnson for calculating typical closing pressures on thermal batteries.

This article has been authored by an employee of National Technology & Engineering Solutions of Sandia, LLC under Contract No. DE-NA0003525 with the U.S. Department of Energy (DOE). The employee owns all right, title and interest in and to the article and is solely responsible for its contents. The United States Government retains and the publisher, by accepting the article for publication, acknowledges that the United States Government retains a non-exclusive, paid-up, irrevocable, world-wide license to publish or reproduce the published form of this article or allow others to do so, for United States Government purposes. The DOE will provide public access to these results of federally sponsored research in accordance with the DOE Public Access Plan https://www.energy.gov/downloads/doe-public-access-plan. This paper describes objective technical results and analysis. Any subjective views or opinions that might be expressed in the paper do not necessarily represent the views of the U.S. Department of Energy or the United States Government.

References

1. www.admet.com/products/universal-testing-machines/expert-2600/
2. C.C. Roberts et al. Experimental Characterization of Mechanical Deformation and Fluid Transport Within Thermal Battery Constituents, SAND2017-8209, Sandia National Laboratories, 2017